

Adaptive Uncertainty Distribution in Deep Learning for Unsupervised Underwater Image Enhancement

Alzayat Saleh*, Marcus Sheaves*, Dean Jerry*[†], and Mostafa Rahimi Azghadi*[†]

*College of Science and Engineering, James Cook University, Townsville, QLD, Australia

[†]ARC Research Hub for Supercharging Tropical Aquaculture through Genetic Solutions, James Cook University, Townsville, QLD, Australia

Abstract—One of the main challenges in deep learning-based underwater image enhancement is the limited availability of high-quality training data. Underwater images are difficult to capture and are often of poor quality due to the distortion and loss of colour and contrast in water. This makes it difficult to train supervised deep learning models on large and diverse datasets, which can limit the model’s performance. In this paper, we explore an alternative approach to supervised underwater image enhancement. Specifically, we propose a novel unsupervised underwater image enhancement framework that employs a conditional variational autoencoder (cVAE) to train a deep learning model with probabilistic adaptive instance normalization (PAdaIN) and statistically guided multi-colour space stretch that produces realistic underwater images. The resulting framework is composed of a U-Net as a feature extractor and a PAdaIN to encode the uncertainty, which we call UDnet. To improve the visual quality of the images generated by UDnet, we use a statistically guided multi-colour space stretch module that ensures visual consistency with the input image and provides an alternative to training using a ground truth image. The proposed model does not need manual human annotation and can learn with a limited amount of data and achieves state-of-the-art results on underwater images. We evaluated our proposed framework on eight publicly-available datasets. The results show that our proposed framework yields competitive performance compared to other state-of-the-art approaches in quantitative as well as qualitative metrics. Code available at <https://github.com/alzayats/UDnet>.

Index Terms—Computer Vision, Convolutional Neural Networks, Underwater Image Enhancement, Variational Autoencoder, Machine Learning, Deep Learning.

I. INTRODUCTION

One of the main challenges faced in deep learning-based underwater image enhancement is the lack of large datasets of high-quality underwater images. Unlike many other domains, such as natural images, there are relatively few high-quality underwater images available for training deep learning models. This makes it challenging to train accurate models for enhancing underwater images. Additionally, the unique properties of water, such as refraction and absorption, make it challenging to apply image enhancement techniques that have been developed for other domains.

An underwater environment is a challenging environment due to the extreme range of colour and contrast, especially when compared to images acquired in controlled environments where a vast majority of existing underwater image enhancement algorithms were trained. When natural light enters the water from the air, it can be scattered multiple times as

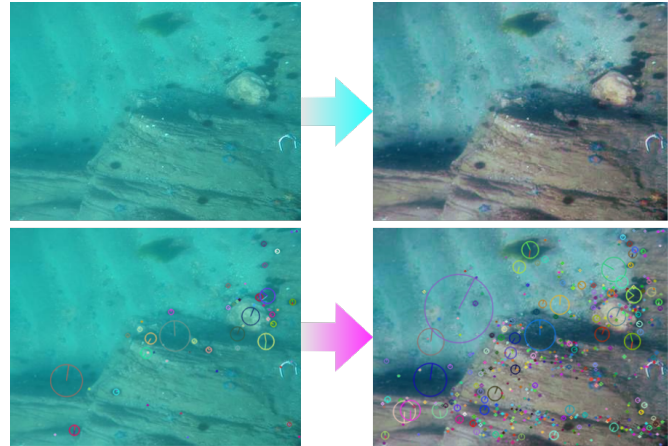


Fig. 1. Our underwater image enhancement model increase underwater robots’ capacity to visually perceive their surroundings. Please refer to Sec. IV-G for details. Best viewed online for colour and details.

it travels through the water. This scattered light forms the background light that illuminates the underwater scene. In addition to the background light, the light that is directly reflected off objects in the scene also travels to the camera. The total light that is perceived by the camera is the sum of these two components: the background light and the directly reflected light. This is what creates the colours and details that we see in underwater images, see Fig. 2 right image. Moreover, different wavelengths of light are absorbed and scattered at different rates as they travel through water. Blue light, with its shorter wavelength, is less absorbed and scattered than other colours, which is why it can travel the longest distance through water. As a result, when we look at objects underwater, the blue light is the most dominant, giving the images a blueish tint, see Fig. 2 left image.

Moreover, objects immersed in water typically appear pale and blurry, making it hard to recognize features. Also, colours are washed out, reducing contrast and visual information. This effect is known as the *aberration of refraction* and it is due to the variation in the refractive index of water as the light passes through it. When light travels from one medium to another, it bends, or refracts, due to the change in the speed of light in the new medium. This can cause the light to be focused at a different point than where it would be focused in the absence of refraction, resulting in distortion of the image. Aberration of refraction is particularly significant in

underwater photography, where the refractive index of water is different from that of air. Due to the refraction, colourful underwater objects appear pale, and contrast is lost between the sea objects and backgrounds.

Furthermore, there is an imbalance between colour channels, causing a problem known as colour cast, which consists of different colours depending on the wavelength range of light that has travelled through the water. This effect is known as *colour cast*, and it is typically caused by incorrect white balance, which is the process of adjusting the colours in an image so that objects that are supposed to be white are actually rendered as white. If the white balance is not correct, the colours in the image may appear unnatural or distorted. Due to these difficulties, underwater image enhancement is a challenging problem that requires specific considerations when implemented. This requires the development of specialized algorithms and techniques for enhancing underwater images.

Underwater image enhancement is a technique used to improve the quality of images taken underwater. This can include correcting for distortion caused by the water, improving colour accuracy, and increasing the overall contrast and sharpness of the image. There are a variety of techniques used for underwater image enhancement, including colour correction, contrast enhancement, and noise reduction.

While traditional image enhancement methods such as histogram equalization do a reasonable job of improving the visual quality of underwater images, current traditional methods struggle with the complexity of underwater images. Despite the difficulties, there is an ever-increasing need for high-quality enhancement of underwater images. For example, underwater robots require high-quality images with proper colour and contrast to accurately perform automated tasks like object detection and target recognition. For example, Fig. 1 shows how the underwater image enhancement model increases underwater robots' capacity to visually perceive their surroundings.

Underwater robots are often used in a variety of applications, including oceanic geological exploration, resource exploitation, ecological research, and others. However, their visual perception is often affected by environmental factors such as water clarity, light conditions, and the presence of particles or other objects in the water. These factors can make it difficult for underwater robots to accurately perceive and interpret their surroundings, which can limit their ability to perform their intended tasks. To overcome this, researchers are developing various approaches to improve the visual perception of underwater robots, such as using advanced imaging sensors [1] and software [2] for image enhancement and object recognition. However, specialized hardware platforms and cameras can be expensive and power-consuming.

Despite the challenges, underwater image enhancement has been an active area of research. Early methods relied on histogram equalization and contrast stretching and were not able to achieve effective results. Recently, much progress has been made in the field of underwater image enhancement. [3–5] showed that convolutional neural network (CNN) based image enhancement algorithms perform well on underwater images, achieving enhanced images with improved contrast

and colour reproduction. The work in [6] introduced a CNN-based image enhancement framework for underwater images that is able to automatically determine optimal parameters for enhancing underwater images, resulting in images with both high quality and low computational cost. This method has achieved state-of-the-art performance compared to prior work in image enhancement for underwater images. However, these methods are not efficient considering they are trained in a supervised manner with a set of potential reference images and manually select the best one as the ground truth.

In this work, we explore an alternative approach to supervised underwater image enhancement. Specifically, we propose a novel unsupervised underwater image enhancement framework that is composed of a U-Net and PAdaIN. The purpose of the network is to learn a better representation of underwater images through a CNN in combination with probabilistic adaptive instance normalization (PAdaIN). The PAdaIN can be viewed as a form of Bayesian feature learning, in which feature learning happens automatically through backpropagation. In contrast to prior work in underwater image enhancement, we use a PAdaIN to transform the global enhancement statistics of input features. We also leverage the PAdaIN to encode uncertainty in the network, which can result in better image quality.

Finally, we develop an iterative multi-scale statistically guided multi-colour space stretch that improves the visual quality of the auto-generated reference image. Multi-scale statistically guided means that the stretch modules adaptively increase the contrast of images by regulating histogram distribution in distinct colour spaces. This is essential to the training process of the proposed model since it needs to both model the uncertainty and the statistical similarity between the input image and the reference image.

Our main contributions are summarized as follows:

- We propose a probabilistic unsupervised underwater image enhancement framework that leverages an encoder-decoder network that learns the enhancement distribution of the underwater images.
- To improve the visual quality of the reference image, we develop a multi-scale statistically guided multi-colour space stretch that improves the visual quality of underwater images by ensuring the colour distribution of the reference image.
- We show that while our method does not need manual human annotation it exceeds the SOTA supervised models on several datasets.

The rest of this paper is organized as follows. In Sec. II, we review the related work on underwater image enhancement. In Sec. III, we describe the proposed PAdaIN, and the multi-scale unsupervised underwater image enhancement framework. We describe the dataset, the experimental setup used in our work, the results of the proposed algorithm, and evaluate our approach in Sec. IV. The detailed discussions of our results are presented in Sec. V. Finally, we provide concluding remarks and future directions for further research in Sec. VI.

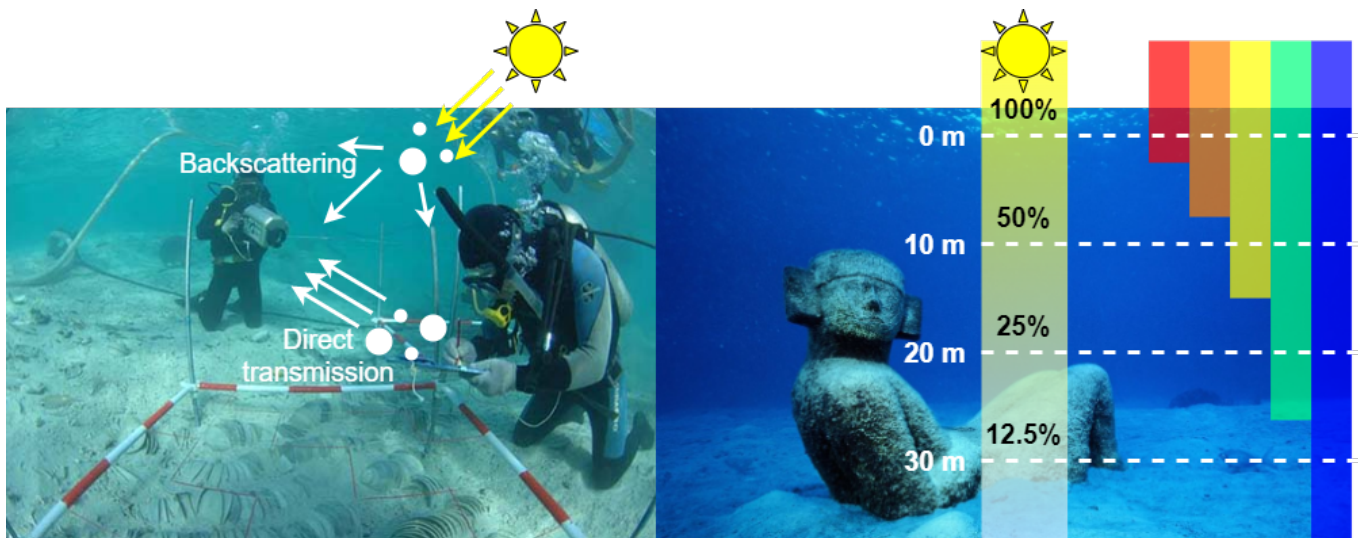


Fig. 2. Natural light entering the water is scattered multiple times, forming the backscattering for the underwater scene. The light directly reflected off objects in the scene also travels to the camera, and the total light perceived is the sum of these two components, creating the colours and details in underwater images, (left). Different wavelengths of light are absorbed and scattered differently as they travel through water. Blue light travels the longest distance due to its shorter wavelength, making underwater objects appear blue in colour, (right). [7]

II. RELATED WORK

Underwater image enhancement is a field of research that focuses on improving the visual quality of images taken beneath the surface of the water. This is a challenging task because water is a highly scattering medium, which means that it diffuses light in many directions and reduces the amount of light that reaches the camera. As a result, images taken underwater often appear blurry, dark, and colourless.

One approach for enhancing underwater images is called prior-based. These methods use physical-model-based to improve the accuracy of image enhancement. Physical-model-based methods aim to improve underwater images by using visual cues to estimate the optical parameters that affect the images. By applying these parameters in reverse, the original, unaltered images can be reconstructed. Examples of the visual cues used in these methods include the red channel prior [8], the underwater dark channel prior [9], and the underwater light attenuation prior [10]. One example of this is the use of a dehazing algorithm proposed by Chiang et al [7]. The Galdran et al. [8] method is a variation of the Dark Channel Prior approach that uses red channel information to calculate the depth of underwater images. Berman et al. [11] looked at using various spectral profiles of various water types and calculated two global parameters: the attenuation ratios of the blue-red and blue-green colour channels. Another prior-based method, called Sea-thru, was developed by Akkaynak et al. [12] and uses RGBD images as input to estimate backscatter and the attenuation coefficient.

Another approach to underwater image enhancement is known as the model-free method. These methods enhance the images without taking into account the degradation process that they have undergone. Examples of such methods include traditional contrast-limited adaptive histogram equalization [13], white balance [14] which adjusts the overall colour balance of an image to compensate for the blueish tint that

is often present in underwater images, and Retinex [15]. In some cases, these methods may be combined or enhanced with additional techniques, such as fusion-based approaches [16] or multi-scale strategies [17], to improve their performance. In other cases, these methods may improve image quality by adjusting pixel values. One example is UCM [18], which is an unsupervised colour correction technique. It uses white balance [14] to even out the different colours, and then it makes the image's contrast higher. Another technique [19], called adaptive histogram enhancement, builds on UCM and uses Rayleigh distribution stretching to make images clearer and reduce over-enhancement. These methods can make underwater images look brighter and clearer.

Deep learning-based methods are the third category of approaches to enhancing underwater images. These methods use training data to automatically extract useful information from the images and apply it to enhance it. These methods can be divided into convolutional neural networks (CNN) [20] and generative adversarial networks (GAN) [21]. One example of the use of the CNN is by Sun et al. [22]. They proposed a CNN model that utilized an encode-decoder framework for removing noise from underwater images. Li et al. [23] developed a lightweight CNN model that incorporates information about the underwater scene to synthesize degraded images. Li et al. [24] also proposed a model that uses information about light transmission to improve the quality of degraded images in specific regions. Another example is the use of a GAN, as proposed by Li et al. [25], to generate synthetic underwater images in an unsupervised manner. This approach allows for the training of an enhancement network using the synthetic data. Another example is the weakly supervised method proposed by Li et al. [26], which reduces the need for paired data. Additionally, Guo et al. [27] enhanced degraded underwater images using a multi-scale dense generative adversarial network. Islam et al. [28] introduced FUnIE-GAN, a

GAN model inspired by U-Net that is effective at improving colour and sharpness in underwater images.

In contrast, our method integrates probabilistic-based methods into deep-learning-based methods, which automatically learn the uncertainty distribution of underwater images. Specifically, our method integrates conditional variational autoencoders (cVAEs). A variational autoencoder (VAE) [29] is a type of deep learning model that is used to generate new data. It is a type of generative model, which means that it can create new data that is similar to the data it was trained on. A VAE consists of two parts: an encoder, which maps the input data to a low-dimensional latent space, and a decoder, which maps the latent space back to the original input space. The encoder and decoder are trained together to maximize the likelihood of the generated data, while also enforcing a regularization constraint on the latent space, which encourages the model to learn a compact and meaningful representation of the input data.

Variational autoencoders (VAEs) [29] and conditional VAEs [30] have been widely used in computer vision tasks. Unlike traditional encoders that output a single value for each latent state attribute, VAEs formulate the encoder to describe a probability distribution for each attribute. To effectively train a VAE, both a regularizer and a reconstruction loss must be implemented. These tools penalize any inconsistencies between the VAE’s posterior and prior distributions of the latent representation. VAEs and cVAEs have been used in a variety of applications related to underwater image enhancement. For instance, in some studies, VAEs were utilized to model the background of images for salient object detection [31], while in others they were employed to learn motion sequence generation [32]. Some researchers [33] have even used VAEs to denoise images and predict multiple deprojected instances of images and videos. Additionally, VAEs have been combined with contrastive learning to identify and enhance salient features [34]. Overall, VAEs have proven to be useful for generating diverse solutions in a variety of settings.

III. METHOD

This section describes our Uncertainty Distribution Network (UDnet) in detail. UDnet is based on probabilistic adaptive instance normalization with the guidance of statistics that learns meaningful distributions of underwater image enhancement. We present the overview architecture of UDnet in Fig. 3.

A. Uncertainty Distribution

The two main modules of UDnet are the statistically guided multi-colour space stretch and the probabilistic adaptive instance normalization (PAdaIN). The statistically guided multi-colour space stretch module adjusts the image’s colour balance, while the PAdaIN module captures and encodes the uncertainty in the enhancement process. The PAdaIN module is trained on a dataset of images and their corresponding reference images, which allows it to learn the posterior distributions of the mean and standard deviation of the image features. In the testing phase, random samples are extracted from these distributions and injected into the PAdaIN module to adjust

the statistics of the received features. This allows UDnet to align the mean and standard deviation of the input image with those of the reference image, resulting in improved image enhancement.

In the context of underwater image enhancement, uncertainty distribution refers to the inherent uncertainty that can exist in the image enhancement process. In order to account for the inherent uncertainty in image enhancement, UDnet introduces Uncertainty Distribution as an implicit variable that represents the various factors that could affect the outcome of the enhancement process. This variable could be related to human subjective preferences, the parameters of the camera or enhancement algorithms used, or any other factors that may influence the final result. By taking this uncertainty into account, UDnet is able to more accurately capture the range of possible enhancements, rather than trying to determine a single “correct” result. This is particularly useful in situations where the true, unaltered image is not available or cannot be accurately reproduced.

It is worth noting that in contrast to other approaches that consider the variance of the image, such as GAN, PAdaIN is based on the statistical distribution of the image features, which are invariant to transformations like colour transformation. This is done by conditioning the network on training images and their reference map, which, along with the use of a differentiable approximation of the uncertainty, make UDnet easily trainable with a single backward pass.

B. Reference Maps Generation

The main challenge when training a probabilistic network for underwater image enhancement is the limited availability of reference maps for degraded images. To address this issue, we auto-generated reference maps based on UIEBD [35], which contains real-world underwater images and corresponding reference maps generated using 12 state-of-the-art enhancement algorithms. In the original UIEBD, volunteers were asked to compare the enhanced results and subjectively select the best one as the final reference image. However, our reference map generation process uses the same intuition without human intervention. Using the degraded image (original image), we generate three enhanced reference maps by three enhancement algorithms to introduce uncertainty into the dataset. It is worth mentioning that adding more enhanced reference maps did not increase the model accuracy as discussed in more detail in Sec. IV-H.

To introduce uncertainty into the dataset, we performed contrast and saturation adjustment, as well as gamma correction on the original images. These methods were chosen because they can effectively simulate the distortions commonly found in underwater images, such as changes, in contrast, saturation, brightness, and colours. As shown in Eq. (1), the contrast and saturation adjustment were performed using a linear transformation formula, where the adjustment coefficient α was the same for all pixels for contrast adjustment and varied for each pixel for saturation adjustment.

$$y = (x - m) \times \alpha + x, \quad (1)$$

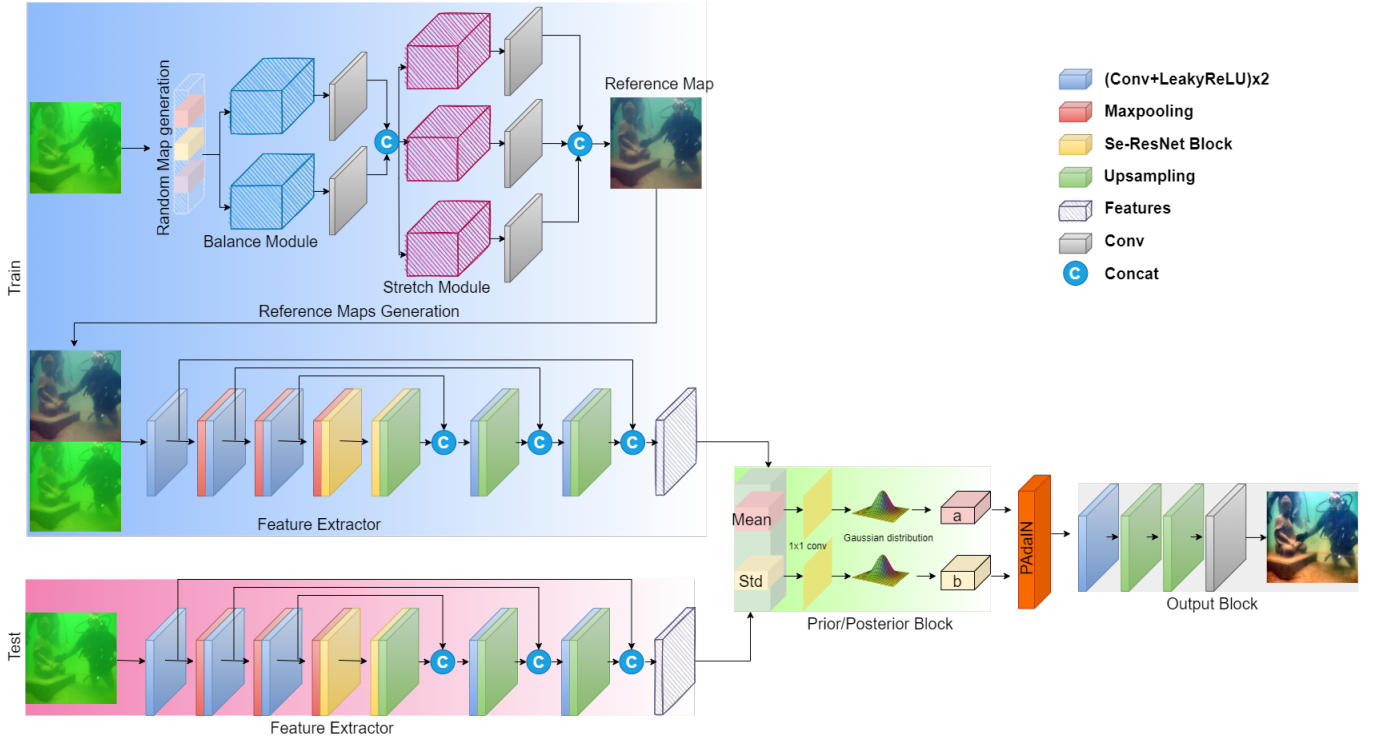


Fig. 3. The architecture of UDnet is composed of two main modules: the reference maps generation module and the features extractor module. The input is a three-dimensional underwater image with pixel values ranging from 0 to 1. UDnet uses a U-Net feature extractor to map input images to representations, which are then transformed by the PAdaIN module to create the enhanced image. In the training phase, the feature extractor is used to calculate the posterior distribution, and random samples from this distribution are used to transform the enhancement representation. In the testing phase, a single degraded image is used as the input and random samples from the Prior block are used to generate the enhanced output image. The detailed structure of each module is described in subsequent subsections of the paper.

where x and y refer to the degraded image and enhanced image, m denotes the mean of each channel. α is the adjustment coefficient.

Our goal was to create uncertain labels that would reflect the uncertainty in the ground truth recording, rather than significantly altering the original labels. Our approach has several advantages, including saving time and increasing reliability compared to using human observers to generate reference maps. We evaluated the effectiveness of the generated reference maps in Sec. IV-E and Sec. IV-F by comparing the enhanced results to the subjective selections made by volunteers in the original UIEBD dataset.

C. Colour Correction Module

The colour correction module's goal is to improve the colour and contrast of the reference map generated in Sec. III-B. This is obtained by transforming the reference map RGB values to the optimal RGB values, which involves determining the proper camera white-balance for colour-neutral subjects, as well as removing the effects of lens flare and red-green chromatic aberration. This could be useful when dealing with oversaturated images. The colour correction module is designed for the case where the mean and standard deviation of the red, green and blue (RGB) colour values are known. This module uses a non-parametric approach to colour correction [36], which is able to accommodate new statistical distributions of the pixel values in the red, green and blue

(RGB) colour channels. The colour correction module consists of two main components: a dual-statistic balance module and a multi-colour space stretch module.

In the dual-statistic balance module, the image is processed by two different modules that use statistics of the image (average and maximum values) to correct its colour balance. The output is then enhanced using two residual-enhancement modules to recover lost details.

The first residual-enhancement module is based on Grey World theory. The Gray World theory is a method for colour correction in images. It is based on the assumption that the average colour of objects in a perfect image is grey, which means that the average values of the R, G, and B channels are equal. This means that the scale factors for each channel, e_R , e_G , and e_B , can be determined using the GW theory:

$$x^{GW} = Conv_{1 \times 1}(x) \otimes \bar{A},$$

where $\bar{A} = [\frac{1}{A_R}, \frac{1}{A_G}, \frac{1}{A_B}] \in \mathbb{R}^{3 \times 1}$, A_c denotes the average value of c channel in the original image, \otimes denotes pixel-wise multiplication.

The second residual-enhancement module is based on the White Patch algorithm. The White Patch algorithm is another method for colour correction in images. It is based on the assumption that the maximum response of the RGB channels in an image is caused by a white patch in the scene. This white patch is assumed to reflect the colour of the light in the scene, so the largest value in the RGB channels is used as the source of light. Based on this hypothesis, the scale factors for

each channel can be expressed as:

$$x^{WP} = Conv_{1 \times 1}(x) \otimes \overline{M},$$

where $\overline{M} = [\frac{1}{\overline{M}_R}, \frac{1}{\overline{M}_G}, \frac{1}{\overline{M}_B}] \in \mathbb{R}^{3 \times 1}$, M_c denotes the maximum value of c channel in original image..

The result is merged and passed to the stretch module as follows:

$$x^{DSB} = Conv_{3 \times 3}(x^{GW}) \oplus Conv_{3 \times 3}(x^{WP}),$$

where x^{DSB} means the result enhanced by the dual-statistic balance module.

In the multi-colour space stretch module, the image is transformed into different colour spaces (HSI and Lab) and processed by a trainable module to improve contrast. The original image is also enhanced and added to the stretched version as follows:

$$x^{final} = Conv_{3 \times 3}(x^r) \oplus Conv_{3 \times 3}(x^h) \oplus Conv_{3 \times 3}(x^l),$$

Where x^r , x^h , x^l denote the histogram stretched pixel value in RGB, HSI, Lab colour spaces, respectively.

The H channel of the HSI colour space is preserved without any changes. The output is then converted back to the RGB colour space and merged together by going through 3×3 convolutional layer and pixel-wise add up. Overall, this technique can improve the visual quality of the reference map that will be passed to the *Probabilistic Module* by correcting colour balance and enhancing contrast.

D. Probabilistic Module

The main idea behind UDnet is to incorporate uncertainty into the underwater image enhancement process. This is motivated by the fact that the true clean image is often unavailable, and that there is a degree of uncertainty in the labels used to train the model. Existing deterministic learning-guided methods are unable to capture this uncertainty, and have to make compromises between different possible enhancement results.

To address this issue, UDnet uses an implicit variable \mathbf{z} to represent the uncertainty in the enhancement process. This variable could represent human subjective preferences, or the parameters of the camera or enhancement algorithms used to capture or generate the ground truth images. The goal of the model is to learn a mapping from the corrupted image \mathbf{x} to the clean image \mathbf{y} that takes into account the uncertainty represented by \mathbf{z} . This can be formalized as follows:

$$p(\mathbf{y}|\mathbf{x}) \approx p(\mathbf{y}|\mathbf{z}_{\max}, \mathbf{x}), \mathbf{z}_{\max} \sim p(\mathbf{z}|\mathbf{x}), \quad (2)$$

where $p(\mathbf{z}|\mathbf{x})$ denotes the distribution of uncertainty, and \mathbf{z}_{\max} denotes the sample with the maximum probability.

Eq. (2) represents the probabilistic framework underlying UDnet. In this equation, $p(\mathbf{y}|\mathbf{z}_{\max}, \mathbf{x})$ is the probability of the clean image \mathbf{y} given the sample with the maximum probability \mathbf{z}_{\max} and the corrupted observation \mathbf{x} . $p(\mathbf{z}|\mathbf{x})$ is the probability of the uncertainty variable given the observation. The goal of the model is to learn these probability distributions from the training data and then use them to generate enhanced images that incorporate uncertainty into the enhancement process. By doing so, UDnet is able to provide users with multiple

alternative enhancement results and can improve the accuracy and reliability of the final enhancement result.

The goal of UDnet is to adjust the appearance of underwater images, such as the colours and contrasts, without altering the content of the image. This is important because it allows the enhanced images to be more visually appealing and easier to interpret, without compromising the integrity of the original image. Therefore, We use a probabilistic adaptive instance normalization (PAdaIN) to capture these properties.

The proposed PAdaIN method [37] is based on the AdaIN algorithm [38], which is commonly used for style transfer in image processing. AdaIN adjusts the mean and standard deviation of the features of the content image to match those of the style image, effectively changing the appearance of the content image without altering its content. This approach is useful for UIE because it allows the model to adjust the appearance of the image without changing its content, which is important for maintaining the integrity of the original image.

However, AdaIN relies on the availability of known content and style images, which is not always the case in UIE. To address this issue, PAdaIN introduces random samples from the posterior distributions of the mean and standard deviation as the parameters of the AdaIN operation, which can be formulated as:

$$PAdaIN(\mathbf{x}) = \mathbf{b} \left(\frac{\mathbf{x} - \boldsymbol{\mu}(\mathbf{x})}{\boldsymbol{\sigma}(\mathbf{x})} \right) + \mathbf{a}, \quad (3)$$

where \mathbf{b} and \mathbf{a} are two random samples from the posterior distributions of the mean and standard deviation, respectively.

These posterior distributions are learned using a CVAE, which will be described in more detail in the next subsection. This allows PAdaIN to generalize the AdaIN algorithm and apply it to UIE without the need for known content and style images. Overall, PAdaIN is able to capture the important appearance-related features of the input image and use them to generate enhanced images that maintain the integrity of the original image.

E. Network Structure

The architecture of UDnet is shown in Fig. 3. The architecture of UDnet is composed of two main modules: the reference maps generation module and the features extractor module. The input to UDnet is a three-dimensional underwater image with pixel values ranging from 0 to 1. The network uses convolutional layers with a kernel size of 3×3 and a stride of 1 to merge enhanced images together. UDnet uses a U-Net feature extractor to map input images to representations. These representations are then fed into the PAdaIN module, which transforms the enhancement statistics of the input to create the enhanced image. In the training phase, the features extractor is used to calculate the posterior distribution, and random samples from this distribution are injected into the AdaIN module to transform the enhancement representation. In the testing phase, a single degraded image is used as the input, and random samples from the Prior block are used to generate the enhanced output image.

The feature extractor module has two branches, which both include a feature extractor based on U-Net. The training branch

is used to construct posterior distributions of UIE using the raw underwater image and a corresponding reference image as input, while The test branch is used to estimate the prior distribution of a single raw underwater image.

The core component of UDnet is the PAdaIN, which is a modified version of the AdaIN algorithm that is specifically designed for use in UIE, as proposed by Fu et. al. [37]. The PAdaIN component is used to encode the uncertainty in the input image, allowing the model to generate multiple enhanced versions of the image that capture the different possible interpretations of the original image.

To achieve this, UDnet uses a prior/posterior block to build the distribution of possible enhancements. This block is designed to construct both a mean and a standard deviation distribution, using 1×1 convolutions to transform the input data matrix into a series of distributions that capture the uncertainty in the input image. In the training stage, the input image and its corresponding reference image are used to learn the posterior distributions of the latent codes as follows:

$$\mathbf{a} \sim \mathcal{N}_m(\boldsymbol{\mu}(\mathbf{y}, \mathbf{x}), \boldsymbol{\sigma}^2(\mathbf{y}, \mathbf{x})), \quad (4)$$

$$\mathbf{b} \sim \mathcal{N}_s(\mathbf{m}(\mathbf{y}, \mathbf{x}), \mathbf{v}^2(\mathbf{y}, \mathbf{x})), \quad (5)$$

where \mathbf{a} and \mathbf{b} are two random samples from the mean and standard deviation posterior distributions, (\mathcal{N}_m) and (\mathcal{N}_s) are the N -dimensional Gaussian distribution of the mean and standard deviation, \mathbf{y} and \mathbf{x} are the clean image and the corrupted observation, respectively.

Once these distributions have been constructed, random samples are extracted from them and injected into the PAdaIN module, where they are used to transform the statistics of the received features.

In the testing stage, the latent codes generated for the PAdaIN are determined only by the input image to learn the prior distributions of the latent codes as follows:

$$\mathbf{a} \sim \mathcal{N}_m(\boldsymbol{\mu}(\mathbf{x}), \boldsymbol{\sigma}^2(\mathbf{x})), \quad (6)$$

$$\mathbf{b} \sim \mathcal{N}_s(\mathbf{m}(\mathbf{x}), \mathbf{v}^2(\mathbf{x})), \quad (7)$$

where \mathbf{a} and \mathbf{b} are two random samples from the mean and standard deviation posterior distributions, (\mathcal{N}_m) and (\mathcal{N}_s) are the N -dimensional Gaussian distribution of the mean and standard deviation, respectively. \mathbf{x} is the corrupted observation.

Then, the UDnet model is applied multiple times to the same input image in order to generate multiple enhancement variants. This is done by re-evaluating only the PAdaIN module and the output block, without retraining the entire model. The resulting diverse enhancement samples are used for Maximum Probability estimation that takes the enhancement sample with the maximum probability as the final estimation.

F. Loss Function

The training process for UDnet follows the standard procedure for training a cVAE model, which involves minimizing the variational lower bound. However, our approach has an additional step of finding a meaningful embedding of enhancement statistics in the latent space. This is achieved through the use of a posterior network (as shown in Fig. 3), which learns

to recognize posterior features and map them to posterior distributions of the mean and standard deviation. Random samples from these distributions can be used to formalize the enhanced results. This approach allows for the incorporation of uncertainty into the enhancement process, which can improve the accuracy and reliability of the resulting images.

During the training process, the AdaIN module is used to predict the enhanced image by feeding it random samples \mathbf{a} and \mathbf{b} from Eq. (4) and Eq. (5), respectively. The enhancement loss (Eq. (8)) is calculated based on the differences between the predicted image and the reference map, and is used to penalize the model if the output deviates from the reference. The exact formula for enhancement loss is:

$$L_e = L_{\text{mse}} + \lambda L_{\text{vgg16}}, \quad (8)$$

where L_{mse} denotes the mean square error loss and L_{vgg16} denotes the perceptual loss [39], λ refers to the weight.

The mean square error loss L_{mse} and the perceptual loss L_{vgg16} are two common metrics used to evaluate the performance of image enhancement algorithms. The mean square error loss measures the average squared difference between the predicted and reference images, while the perceptual loss, which was introduced by Johnson et al. [39], measures the differences between the high-level features of the predicted and reference images. The weight λ is used to control the relative importance of these two loss terms in the overall enhancement loss L_e . For example, if λ is set to a high value, the model will be more heavily penalized for large differences between the predicted and reference images, while if λ is set to a low value, the model will be less sensitive to such differences. The specific values of λ used in the training process will depend on the characteristics of the dataset and the desired performance of the model.

In addition to minimizing the enhancement loss L_e , the training process for UDnet also involves using Kullback-Leibler (KL) divergences D_{KL} to align the posterior distributions with the prior distributions (Eq. (9) and (Eq. (10)). KL divergences is a measure of the difference between two probability distributions and can be used to compare the posterior distributions learned by the model with the prior distributions that are assumed to represent the distribution of latent variables in the training data. By minimizing the KL divergences between the posterior and prior distributions, the model is able to learn a more accurate representation of the latent space, which can improve the quality of the enhanced images. The exact formula for Kullback-Leibler (KL) divergences is:

$$L_m = D_{\text{KL}}(\mathcal{N}_m(\mathbf{x}) \parallel \mathcal{N}_m(\mathbf{y}, \mathbf{x})), \quad (9)$$

$$L_s = D_{\text{KL}}(\mathcal{N}_s(\mathbf{x}) \parallel \mathcal{N}_s(\mathbf{y}, \mathbf{x})), \quad (10)$$

where \mathbf{m} and \mathbf{s} are the mean and the standard deviation, respectively.

The total loss function used for training UDnet is the weighted sum of the enhancement loss L_e and the KL divergences D_{KL} between the posterior and prior distributions:

$$L = L_e + \beta(L_m + L_s), \quad (11)$$

where β is the weight.

The specific weight β used for these loss terms will depend on the dataset’s characteristics and the model’s desired performance. By minimizing this total loss function, the model is able to learn an effective mapping from the input degraded images to the corresponding enhanced images, while also aligning the posterior and prior distributions in the latent space. This allows the model to generate high-quality enhanced images while also incorporating uncertainty into the enhancement process.

IV. EXPERIMENTS

In this section, we perform several experiments to evaluate the performance of our proposed method. We will first describe the datasets, evaluation metrics and implementation details. Then, we quantitatively and qualitatively evaluate our model against 10 popular image enhancement models on 8 public datasets. Finally, we will demonstrate the significance of our work through a visual perception improvement test.

A. Datasets

We used eight publicly available datasets for our model’s performance verification. These datasets are: EUVP [28], UFO [40], UIEBD [35], DeepFish [41], FISHTRAC [42], FishID [43], RUIE [44], SUIM [45]. Details of these datasets can be found in Table I. In EUVP [28], UFO [40], and UIEBD [35], there are many paired images and unpaired images which were divided as shown in Table I. The paired images are the ones that have ground truth. The rest of the datasets have only unpaired images. In our experiment, we used only UIEBD [35] for training in an unsupervised way without the ground truth and the other datasets for performance evaluation.

TABLE I
THE DATASETS USED IN OUR RESEARCH. THE NUMBERS
REPRESENTS THE AMOUNT OF IMAGES IN SETS

Datasets	Train		Test	
	Paired	Unpaired	Paired	Unpaired
EUVP [28]	3700	3140	515	-
UFO [40]	1500	-	120	-
UIEBD [35]	800	-	90	60
DeepFish [41]	-	3200	-	600
FISHTRAC [42]	-	600	-	71
FishID [43]	-	7093	-	6897
RUIE [44]	-	2904	-	726
SUIM [45]	-	1525	-	110

B. Evaluation Metrics

Evaluation metrics for image enhancement are often based on natural image statistics. Perceptual and structural image qualities can be judged in different ways. We employ four full-reference evaluation metrics and three no-reference evaluation metrics for evaluating the quantitative performance

of our image enhancement model. Specifically, 1) The full-reference evaluation metrics consist of Peak Signal-to-Noise Ratio (PSNR) [46], Structural Similarity (SSIM) [46], Most Apparent Distortion (MAD) [47], and Gradient Magnitude Similarity Deviation (GMSD) [48], which are used for paired test sets (EUVP [28], UFO [40], UIEBD [35]). A higher PSNR or a lower MAD score means that the output image and the label image are closer in perceptual content, while a higher SSIM or a lower GMSD score means that the two images are more structurally similar. 2) The no-reference evaluation metrics are: Underwater Image Quality Measure (UIQM) [49], Multi-scale Image Quality Transformer (MUSIQ) [50], and Natural Image Quality Evaluator (NIQE) [51] which are used for unpaired test sets (DeepFish [41], FISHTRAC [42], FishID [43], RUIE [44], SUIM [45]). The UIQM is the linear combination of three underwater image attribute measures: the underwater image colourfulness measure (UICM), the underwater image sharpness measure (UISM), and the underwater image contrast measure (UIConM). A higher UIQM and MUSIQ or a lower NIQE score suggests a better human visual perception. However, it is worth noting that these no-reference metrics cannot accurately reflect the quality of an image in some cases [52] [53], so scores of UIQM, MUSIQ and NIQE are only provided as references for our study. We will present enhanced unpaired images in the visual comparisons section for readers to appraise.

C. Implementation Details

Our models were trained with an input resolution of 256×256 pixels. We scale the lowest side of the image to 256 and then extract random crops of size 256×256 . We found that for this problem set, a learning rate of 1×10^{-4} works the best. It took around 500 epochs for the model to train on this problem and the batch size was set as 10. Our networks were trained on a Linux host with a single NVidia GeForce RTX 2080 Ti GPU with 11 GB of memory, using Pytorch framework [54]. The training is carried out with ADAM optimizer, and the loss functions are the Mean Squared Error (MSE) L_{mse} , the perceptual loss [39] L_{vgg16} and Kullback-Leibler (KL) divergences [55] L_{kl} .

In order to boost network generalisation, we augment the training data with rotation, flipping horizontally and vertically. Following [37], we adopt 1×1 convolutions to broadcast the samples to the desired number of channels before input to AdaIN with a latent space of a 20-dimensional N .

D. Compared Methods

We selected ten works to make fair comparisons with our model, including six conventional unsupervised methods (CLAHE [56], IBLA [57], RGHS [58], UCM [18], UDCP [9], ULAP [10]) and four deep-learning-based methods (PIFM [59], PUIenet [37], USLN [6], Wavenet [60]). The comparison with conventional unsupervised methods aims to demonstrate the advantages of our trainable unsupervised deep-learning-based method.

We applied these conventional unsupervised approaches directly to the test sets. We used the authors’ code and

TABLE II
COMPARISON AGAINST PUBLISHED WORKS ON THREE PAIRED DATASETS (EUVP [28], UFO [40] AND UIEBD [35]).
UNDERWATER IMAGE ENHANCEMENT PERFORMANCE METRIC IN TERMS OF AVERAGE PSNR [46], SSIM [46], MAD [47] AND
GMSD [48] VALUES, (↑) HIGHER IS BETTER, (↓) LOWER IS BETTER. WE REPRESENT THE BEST TWO RESULTS IN RED AND BLUE
COLOURS.
* THE MODEL TRAINED ON UIEBD [35] DATASET WITH LABEL.

Method	EUVP				UFO				UIEBD			
	PSNR ↑	SSIM ↑	MAD ↓	GMSD ↓	PSNR ↑	SSIM ↑	MAD ↓	GMSD ↓	PSNR ↑	SSIM ↑	MAD ↓	GMSD ↓
CLAHE	18.97	0.726	138.6	0.090	18.76	0.701	143.7	0.098	20.64	0.821	100.9	0.053
IBLA	22.62	0.719	97.78	0.068	20.71	0.671	122.6	0.082	17.56	0.614	141.2	0.126
PIFM*	20.17	0.747	113.5	0.0719	20.63	0.728	118.2	0.076	23.62	0.852	80.80	0.056
PUIenet*	21.01	0.770	94.55	0.052	21.38	0.737	102.3	0.057	23.74	0.844	79.36	0.057
RGHS	21.13	0.753	98.40	0.056	20.74	0.730	112.8	0.066	23.57	0.803	81.02	0.053
UCM	20.91	0.767	99.37	0.062	20.34	0.743	110.0	0.068	22.03	0.815	92.95	0.067
UDCP	15.80	0.572	136.8	0.098	15.95	0.561	148.1	0.111	13.47	0.548	139.0	0.118
ULAP	21.91	0.730	108.4	0.071	21.98	0.729	116.7	0.071	18.95	0.718	113.0	0.085
USLN*	20.87	0.771	94.62	0.050	20.73	0.749	105.0	0.057	24.04	0.849	78.91	0.057
Wavenet*	20.25	0.753	109.3	0.067	20.98	0.736	115.1	0.071	24.61	0.881	68.08	0.045
UDnet (ours)	22.96	0.771	87.67	0.049	22.43	0.738	99.53	0.053	22.23	0.812	74.21	0.043

training approach for these deep learning-based methods. To guarantee the experiment’s objectivity, we trained the four deep-learning-based methods on UIEBD [35] and applied the author-provided model and network training parameters.

E. Quantitative Comparisons

The comparison results for all paired test sets are summarized in Table II. We report the average scores of the four full-reference metrics (PSNR, SSIM, MAD, GMSD). Table II demonstrates that our proposed method outperforms all six conventional unsupervised methods and all four deep-learning-based methods in all four full-reference metrics on EUVP dataset and almost the same on UFO dataset. Our model achieves the highest PSNR, SSIM scores on EUVP and the lowest MAD, GMSD scores on EUVP, UFO. In addition, we also found that 1) although our model was trained in an unsupervised way, our method still performs better than the fully supervised deep-learning-based models trained on UIEBD dataset on EUVP and UFO. 2) this comparison result shows that our proposed unsupervised deep-learning-based method is better than conventional ones at preserving structural information and contrast preservation, which suggests the superiority of our trainable model. 3) Our model is slightly lower than fully supervised methods on UIEBD dataset. However, this is because fully supervised methods were trained on the images and ground truth labels acquired from the UIEBD. 4) Even without any extra labels, our model outperforms models that are trained on the UIEBD dataset on the two metrics of MAD and GMSD for paired datasets.

We also provided quantitative comparisons for unpaired test sets in Table III. Table III demonstrates that our model gets the highest NIQE on (FISHTRAC, FishID, RUIE, SUIM), and the second-best UIQM score on (DeepFish, FISHTRAC, SUIM). There are some appealing outcomes from Table III, 1) Deep-learning-based models have not outperformed conventional approaches in no-reference evaluation metrics, in contrast to full-reference evaluation metrics. 2) The quantitative results suggest that our method can generalise well on unseen datasets even without ground truth.

F. Qualitative Comparisons

Underwater images possess several unique characteristics. They have more texture content and low luminance and contrast compared to natural images with more texture content and low luminance and contrast. Therefore, it is important to assess human visual perception in terms of image content enhancement in underwater image enhancement, especially for underwater colour enhancement. In order to gain more insights into the effectiveness of our proposed image enhancement method, UDnet, we demonstrate an example of comparing our proposed model with ten popular underwater image enhancement methods (CLAHE [56], IBLA [57], RGHS [58], UCM [18], UDCP [9], ULAP [10], PIFM [59], PUIenet [37], USLN [6], Wavenet [60]) on eight publicly available datasets (EUVP [28], UFO [40], UIEBD [35], DeepFish [41], FISHTRAC [42], FishID [43], RUIE [44], SUIM [45]).

We first present raw images and enhanced images in paired datasets in Fig. 4. This figure shows a sample comparison

TABLE III
COMPARISON AGAINST PUBLISHED WORKS ON FIVE UNPAIRED DATASETS (DEEPFISH [41], FISHTRAC [42], FISHID [43], RUIE [44], AND SUIM [45]).

UNDERWATER IMAGE ENHANCEMENT PERFORMANCE METRIC IN TERMS OF AVERAGE UIQM [49], MUSIQ [50] AND NIQE [51] VALUES, (↑) HIGHER IS BETTER, (↓) LOWER IS BETTER. WE REPRESENT THE BEST TWO RESULTS IN RED AND BLUE COLOURS.

Method	DeepFish			FISHTRAC			FishID			RUIE			SUIM		
	UIQM↑	MUSIQ↑	NIQE↓	UIQM↑	MUSIQ↑	NIQE↓	UIQM↑	MUSIQ↑	NIQE↓	UIQM↑	MUSIQ↑	NIQE↓	UIQM↑	MUSIQ↑	NIQE↓
CLAHE	3.136	25.67	4.10	2.686	48.94	3.78	2.631	37.01	5.20	3.028	34.98	4.48	2.914	58.40	3.66
IBLA	1.993	43.34	6.31	1.704	55.36	6.20	1.745	44.45	6.69	2.577	32.60	4.68	1.839	58.17	4.10
PIFM	3.275	27.39	4.29	2.892	48.38	4.17	2.424	41.14	5.12	3.087	33.29	4.51	2.694	58.56	3.82
PUIenet	3.209	28.82	4.10	3.421	48.60	4.22	2.301	40.08	5.32	3.102	28.32	4.56	2.838	60.03	3.75
RGHS	3.150	42.26	6.72	1.913	57.03	5.57	1.823	44.46	5.95	2.991	30.49	4.32	2.317	59.55	3.75
UCM	2.918	41.37	6.45	2.575	54.39	11.25	2.452	44.32	6.06	3.107	32.59	4.19	2.804	58.51	3.90
UDCP	2.391	42.42	5.72	1.622	51.01	6.09	1.320	37.97	6.48	2.159	29.79	4.71	1.731	56.14	4.09
ULAP	2.814	40.46	6.16	1.763	54.37	6.18	2.176	45.12	5.98	2.396	33.00	4.72	2.232	58.36	3.97
USLN	3.015	32.12	4.24	3.316	49.97	4.30	2.067	44.58	6.32	3.068	32.78	4.44	2.682	61.30	4.03
Wavenet	3.304	40.14	3.00	3.071	56.79	3.70	2.252	46.66	5.15	3.081	30.79	4.56	2.773	61.03	3.67
UDnet(ours)	3.292	24.56	4.02	3.390	50.24	3.41	2.303	37.85	5.11	3.154	26.74	4.18	2.875	57.84	3.65

between the output images generated by our model and those by the ten methods mentioned above. This comparison has a two-fold purpose: (1) to demonstrate the effectiveness of the deep-learning-based methods in the no-reference settings. 2) To demonstrate the superiority of our method, which has enhanced the underwater scenes without ground truth for training.

Furthermore, to prove the superiority of our model in handling unpaired images, we show visual comparisons of randomly selected underwater images from five different datasets in Fig. 5, and Fig. 6, these datasets are much more challenging. We also include a short video of our model’s prediction at <https://youtu.be/k4ASsGze5p8> and https://youtu.be/NV5GH-GG_3c. As Fig. 5 shown, the obvious light limitation of the raw image results in low contrast. For example, UDCP and ULAP models tend to make the image darker, some models even introduce reddish colour, e.g. UCM. In comparison, our model increases both brightness and contrast, making the details of the image clear. Fig. 6 suffers from obvious green deviation, most compared methods cannot achieve satisfactory results. For example, CLAHE, IBLA, and ULAP fail to remove the green deviation. In comparison, our model removes the greenish colour and makes the colour balanced.

Our comparison results show the following: 1) The ground truth label of the paired images has been added to enhance visual quality. However, some of these methods have suffered from problems such as over-enhancement, lack of contrast, and saturation. 2) Some of the paired images have an over-enhanced background, while some have an under-enhanced background, and some have a background of no change.

However, the output image of our model has not shown such problems. 3) Some of the background pixels are saturated. However, our model has not suffered from the over- or under-saturation problem.

G. Visual Perception Improvement

The objective of underwater image enhancement is to increase underwater robots’ capacity to visually perceive their surroundings. Visual perception is extremely important for robots to make autonomous decisions in complex underwater scenarios. We used feature detection and matching to assess the capability of our model to improve the visual perception of underwater images. Feature detection and matching are commonly used techniques in many computer vision applications, such as structure-from-motion, image retrieval, object detection, and image stitching.

We selected two consecutive frames from RUIE [44] dataset, (blue_01.jpg) and (blue_02.jpg), and then enhanced them with our model. The two original images and two enhanced images are matched using SIFT [61] and RANSAC [62]. SIFT stands for Scale-Invariant Feature Transform, which helps locate the local features in an image (keypoints). while RANSAC stands for Random Sample Consensus and is used to match feature points.

Our experimental results show that the numbers of matched points are 74 before the enhancement and 594 after the enhancement. Fig. 7 shows the comparison of image feature point matching before image enhancement and after image enhancement. As can be seen, the enhanced images have more matching points than the original images, which further



Fig. 4. Visual comparisons on challenging underwater images sampled from EUVP [28], UFO [40], and UIEBD [35]. The name on the right of each row refers to the method.

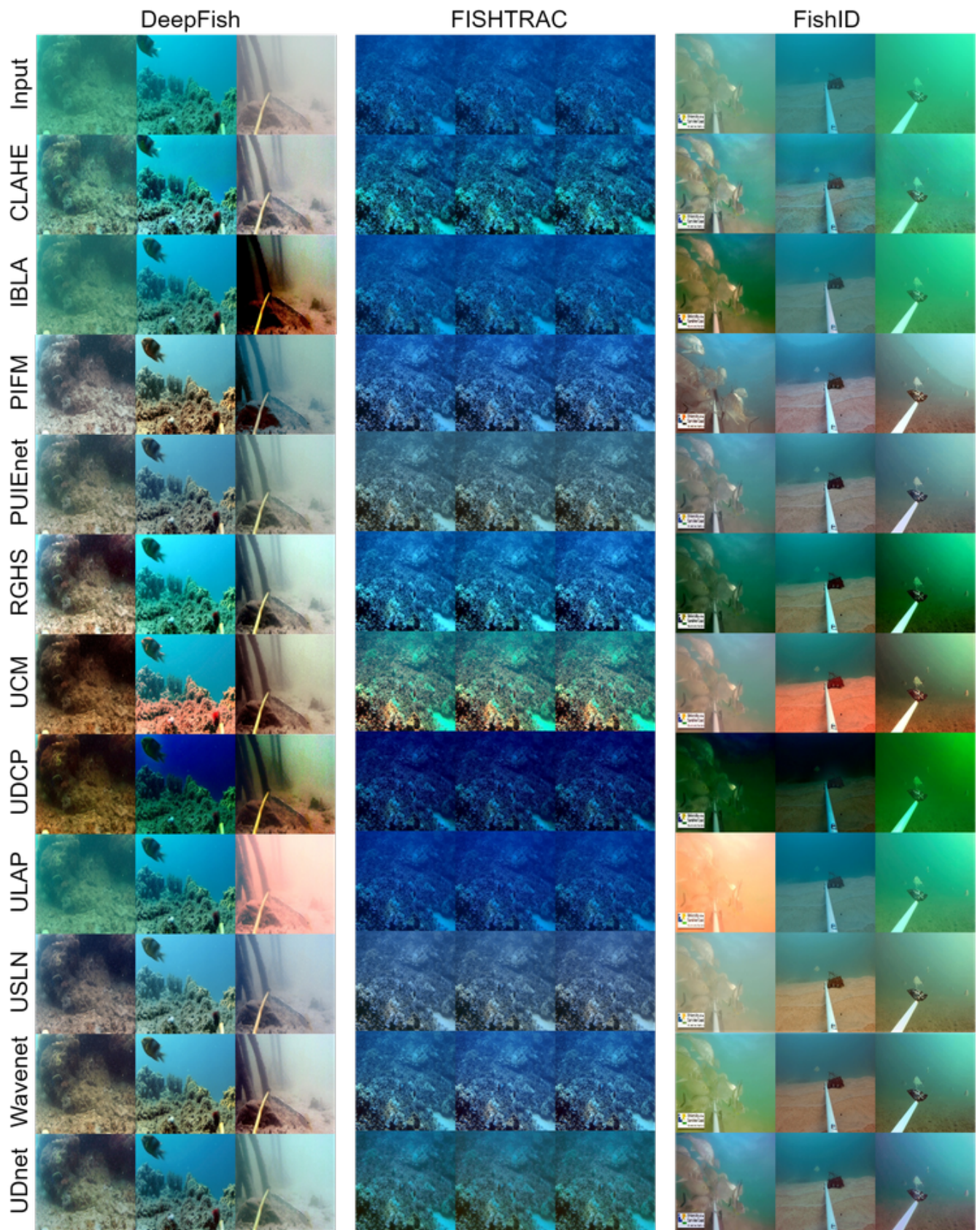


Fig. 5. Visual comparisons on challenging underwater images sampled from DeepFish [41], FISHTRAC [42], and FishID [43]. The name on the right of each row refers to the method. We also include a short video of our model's prediction at <https://youtu.be/k4ASsGze5p8> and https://youtu.be/NV5GH-GG_3c.

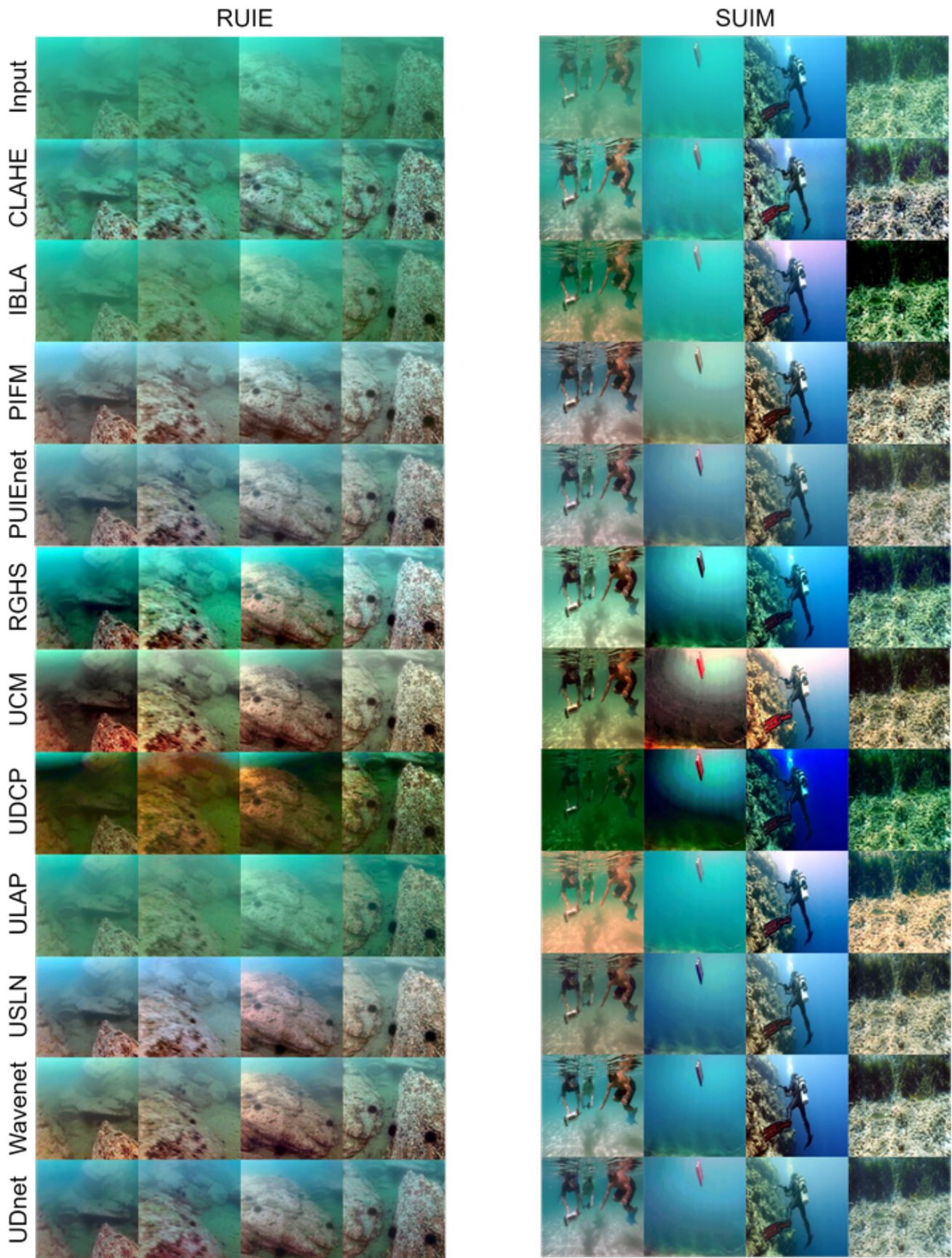


Fig. 6. Visual comparisons on challenging underwater images sampled from RUIE [44], and SUIM [45]. The name on the right of each row refers to the method.

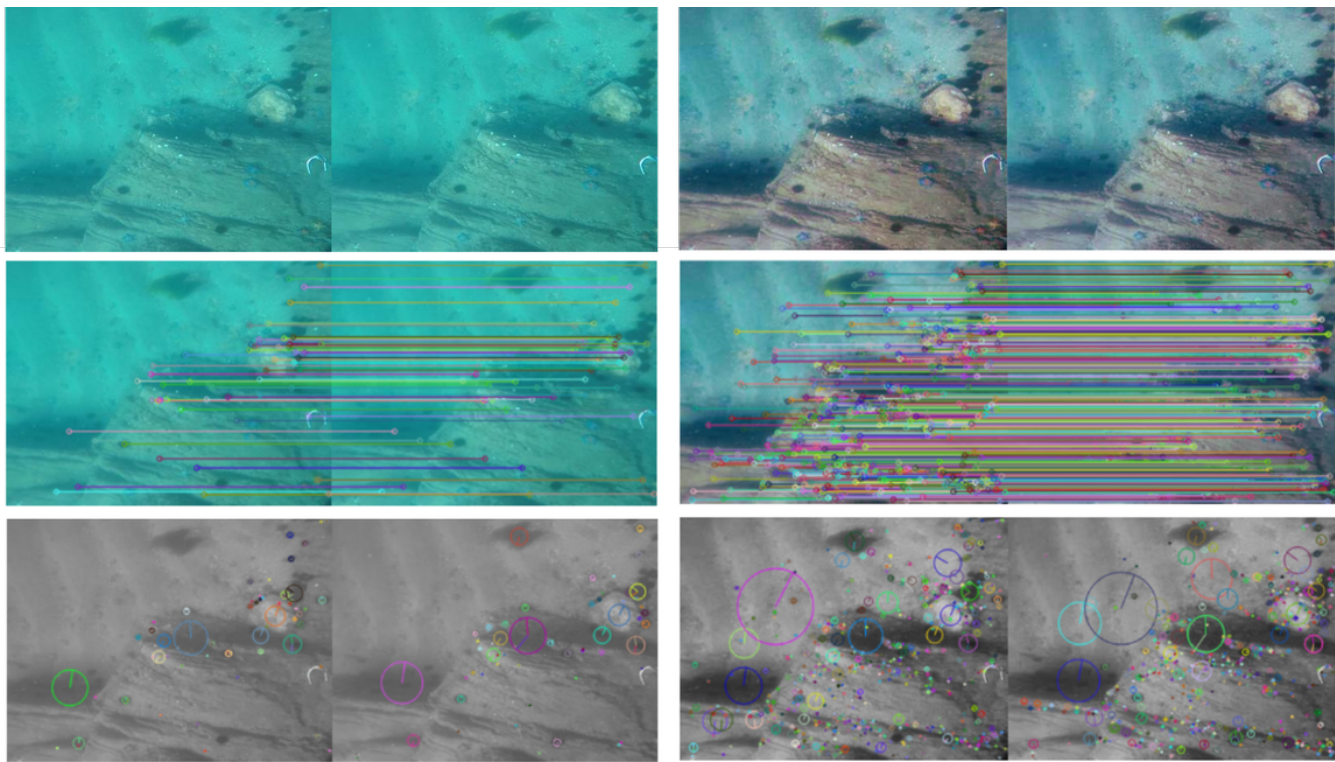


Fig. 7. Comparison of image feature point matching before (left) and after (right) image enhancement with our model. From the top: the original images, matched feature points, and SIFT keypoints. The images are from RUEIE [44] dataset.

demonstrates the efficiency of the image enhancement technique.

H. Ablation Study

For a more in-depth analysis of the proposed method, we analysed the effect of multiple stages of the proposed framework, including the colour module, the new labels generated, and VGG loss. The quantitative comparisons is presented in Table IV, more specifically,

- **w/o colour** means that UDnet is trained without a colour module.
- **All colour** means that UDnet is trained with a colour module in all inputs, not just the label stage.
- **Multi-label** means that UDnet is trained with 6 new generated labels.
- **w/o VGG** means that UDnet is trained without VGG loss.

We used PSNR, and SSIM to evaluate the results on UIEBD, which are shown in Table IV. Compared to the ablation models, the full model achieves the best quantitative performance on both metrics. The qualitative comparisons of the contributions of the colour module, VGG loss, and generated labels are presented in Fig. 8. The conclusions drawn from the ablation study for each contribution are listed as follows:

- 1) Without the colour module, the proposed model gets an unsatisfactory result, see Fig. 8(c). The enhanced image still has low contrast. For example, it has no contrast at the bottom of the image and in the green part, both belong to the sea bed region.

TABLE IV
ABLATION STUDY: COMPARISON AGAINST DIFFERENT BASELINES ON UIEBD DATASET IN TERMS OF AVERAGE PSNR AND SSIM VALUES

Baselines	PSNR \uparrow	SSIM \uparrow
w/o colour	22.01	0.791
All colour	21.73	0.784
Multi-label	22.12	0.795
w/o VGG	21.89	0.789
Full Model	22.23	0.812

- 2) With the colour module in all inputs, the model performs better, see Fig. 8(d). The image is not as dark as (w/o colour). However, the model still under-enhances the detailed information at the bottom of the image and the green parts.
- 3) With the multi labels generated, the quality of the output images not improves, see Fig. 8(e). It reveals that adding more labels than contrast, saturation adjustment, and gamma correction will reduce the performance behind a certain level.
- 4) When UDnet is trained without VGG loss, the quality of the generated image is degraded, see Fig. 8(f). The reduced performance as presented in Table IV demonstrates that the VGG loss can make the model learn more information about the original underwater scene from the labels and improve the visual quality of output.

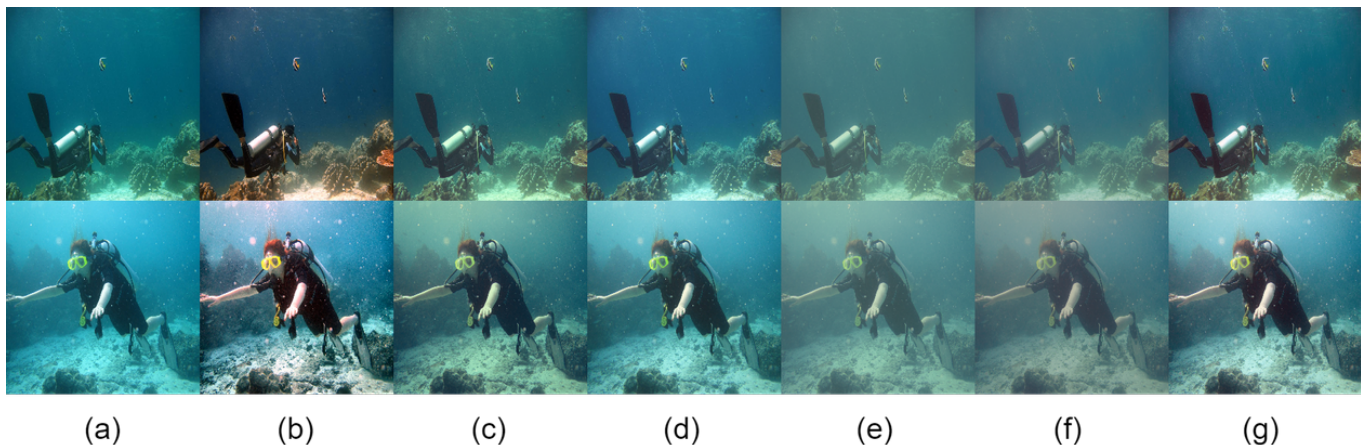


Fig. 8. ABLATION STUDY: The qualitative comparison of the contributions of multiple stages of the proposed framework on the UIEBD dataset. (a) Input, (b) ground truth, (c) w/o colour, (d) All colour, (e) Multi-label, (f) w/o VGG, (g) Full Model.

V. DISCUSSION

A variety of deep learning-based techniques have been proposed to enhance underwater images. Most of these techniques are based on supervised learning that requires a large amount of manually labelled ground truth images. In this work, we propose a novel unsupervised underwater image enhancement framework, which leverages an encoder-decoder network that learns the enhancement distribution of the images. This enables the network to adaptively enhance the input image at training time using a stochastic approach to uncertainty estimation. The proposed method works by adaptively enhancing the input image with the statistical information of a randomly selected reference image at train time. We leverage the probabilistic formulation of a reference image to obtain a more robust enhancement of an image.

The potential applications of this approach for automatically generating reference maps for training probabilistic networks for underwater image enhancement are broad and varied. For example, improved accuracy and reliability of underwater image enhancement could be beneficial in a range of fields, including:

- Environmental monitoring: Better-quality underwater images could be used to track changes in marine ecosystems, such as coral reefs, and monitor the health of aquatic species.
- Marine biology: Enhanced underwater images could provide more detailed information about the behaviour and habitats of marine animals, which could be useful for research and conservation efforts.
- Underwater archaeology: Improved image quality could make it easier to identify and study artifacts and structures in underwater archaeological sites.

In addition to these applications, the approach could also be extended to other domains where reference maps are difficult to obtain, such as medical imaging or satellite image enhancement. In medical imaging, for example, reference maps are often difficult to obtain due to the complexity and variability of human anatomy. Automatically generated reference maps could help to improve the accuracy and reliability of medical

image enhancement, which could be beneficial for diagnostic and therapeutic purposes. Similarly, in the field of satellite image enhancement, reference maps are often difficult to obtain due to the large spatial and temporal scales involved. Automatically generated reference maps could improve the accuracy and reliability of satellite image enhancement, which could be useful for applications such as environmental monitoring and disaster response.

The reference image generation strategy used in our network has a limitation that affects its performance: the difficulty in completely removing backscatter [52], particularly at far distances. We have used state-of-the-art image enhancement algorithms to process raw underwater images, but backscatter can still be present in some cases. While the dataset used in this work is not dominated by such images, backscatter is always discouraged in the reference images. Additionally, some existing algorithms use inaccurate image formation models or assumptions that inherently limit the performance of underwater image enhancement.

In future work, we plan to improve the visual quality of enhanced images and the accuracy of reference maps by using a multi-resolution approach. This strategy involves capturing different types of features in the underwater environment at various resolutions. This can help to improve the overall image quality and better capture the nuances of the underwater environment.

VI. CONCLUSION

We demonstrate that underwater images with the characteristics of random distortion and low contrast are a difficult problem for image enhancement. Our work addresses the challenges in underwater image enhancement by providing an unsupervised approach. We present a fully trainable framework to enhance underwater images without ground truth. We demonstrate that our proposed model outperforms ten popular underwater image enhancement methods on seven common metrics, in both paired and unpaired settings. In addition, as the ground truth labels of unpaired datasets are not publicly available, this study has validated that our proposed model

has an excellent generalisation ability in handling unpaired datasets without using ground truth. In future work, we will explore the effectiveness of other CNN architectures in the underwater image enhancement problem.

ACKNOWLEDGEMENT

This research is supported by the Australian Research Training Program (RTP) Scholarship and Food Agility HDR Top-Up Scholarship. D. Jerry and M. Rahimi Azghadi acknowledge the Australian Research Council through their Industrial Transformation Research Hub program.

REFERENCES

- [1] C. Tan, G. Seet, A. Sluzek, and D. He, "A novel application of range-gated underwater laser imaging system (ULIS) in near-target turbid medium," *Optics and Lasers in Engineering*, vol. 43, no. 9, pp. 995–1009, 9 2005. [Online]. Available: <https://linkinghub.elsevier.com/retrieve/pii/S0143816604002386>
- [2] R. Singh and M. Biswas, "Adaptive histogram equalization based fusion technique for hazy underwater image enhancement," in *2016 IEEE International Conference on Computational Intelligence and Computing Research (ICIC)*. IEEE, 12 2016, pp. 1–5. [Online]. Available: <http://ieeexplore.ieee.org/document/7919711/>
- [3] Y. Lai, Z. Zhou, B. Su, Z. Xuanyuan, J. Tang, J. Yan, W. Liang, and J. Chen, "Single underwater image enhancement based on differential attenuation compensation," *Frontiers in Marine Science*, vol. 9, 11 2022.
- [4] Y. Wang, J. Guo, H. Gao, and H. Yue, "UIEC²-Net: CNN-based underwater image enhancement using two color space," *Signal Processing: Image Communication*, vol. 96, p. 116250, 8 2021. [Online]. Available: <https://linkinghub.elsevier.com/retrieve/pii/S0923596521001004>
- [5] Z. Huang, J. Li, and Z. Hua, "Underwater image enhancement via LBPbased attention residual network," *IET Image Processing*, vol. 16, no. 1, pp. 158–175, 1 2022. [Online]. Available: <https://onlinelibrary.wiley.com/doi/10.1049/ipr2.12341>
- [6] Z. Xiao, Y. Han, S. Rahardja, and Y. Ma, "USLN: A statistically guided lightweight network for underwater image enhancement via dual-statistic white balance and multi-color space stretch," 9 2022. [Online]. Available: <https://arxiv.org/abs/2209.02221v1>
- [7] J. Y. Chiang and Y.-C. Chen, "Underwater image enhancement by wavelength compensation and dehazing," *IEEE transactions on image processing*, vol. 21, no. 4, pp. 1756–1769, 2011.
- [8] A. Galdran, D. Pardo, A. Picón, and A. Alvarez-Gila, "Automatic red-channel underwater image restoration," *Journal of Visual Communication and Image Representation*, vol. 26, pp. 132–145, 2015.
- [9] P. Drews, E. Nascimento, F. Moraes, S. Botelho, and M. Campos, "Transmission estimation in underwater single images," in *Proceedings of the IEEE international conference on computer vision workshops*, 2013, pp. 825–830.
- [10] W. Song, Y. Wang, D. Huang, and D. Tjondronegoro, "A rapid scene depth estimation model based on underwater light attenuation prior for underwater image restoration," in *Pacific Rim Conference on Multimedia*, 2018, pp. 678–688.
- [11] D. Berman, T. Treibitz, and S. Avidan, "Diving into hazelines: Color restoration of underwater images," in *Proc. British Machine Vision Conference (BMVC)*, vol. 1, no. 2, 2017.
- [12] D. Akkaynak and T. Treibitz, "Sea-thru: A method for removing water from underwater images," in *Proceedings of the IEEE Conference on Computer Vision and Pattern Recognition (CVPR)*, 2019, pp. 1682–1691.
- [13] S. M. Pizer, R. E. Johnston, J. P. Ericksen, B. C. Yankaskas, and K. E. Muller, "Contrast-limited adaptive histogram equalization: speed and effectiveness," in *Proceedings of the First Conference on Visualization in Biomedical Computing*, 1990, pp. 337–345.
- [14] Y. C. Liu, W. H. Chan, and Y. Q. Chen, "Automatic white balance for digital still camera," *IEEE Transactions on Consumer Electronics*, vol. 41, no. 3, pp. 460–466, 1995.
- [15] Z.-u. Rahman, D. J. Jobson, and G. A. Woodell, "Multi-scale retinex for color image enhancement," in *Proceedings of 3rd IEEE international conference on image processing*, vol. 3, 1996, pp. 1003–1006.
- [16] C. Ancuti, C. O. Ancuti, T. Haber, and P. Bekaert, "Enhancing underwater images and videos by fusion," in *Proceedings of the IEEE Conference on Computer Vision and Pattern Recognition (CVPR)*, 2012, pp. 81–88.
- [17] C. O. Ancuti, C. Ancuti, C. D. Vleeschouwer, and P. Bekaert, "Color balance and fusion for underwater image enhancement," *IEEE Trans. Image Process.*, vol. 27, no. 1, pp. 379–393, 1 2018.
- [18] K. Iqbal, M. Odetayo, A. James, R. A. Salam, and A. Z. H. Talib, "Enhancing the low quality images using unsupervised colour correction method," in *2010 IEEE International Conference on Systems, Man and Cybernetics*, 2010, pp. 1703–1709.
- [19] A. S. A. Ghani and N. A. M. Isa, "Enhancement of low quality underwater image through integrated global and local contrast correction," *Applied Soft Computing*, vol. 37, pp. 332–344, 2015.
- [20] Y. LeCun, L. Bottou, Y. Bengio, P. Haffner, and others, "Gradient-based learning applied to document recognition," *Proceedings of the IEEE*, vol. 86, no. 11, pp. 2278–2324, 1998.
- [21] I. Goodfellow, J. Pouget-Abadie, M. Mirza, B. Xu, D. Warde-Farley, S. Ozair, A. Courville, and Y. Bengio, "Generative Adversarial Nets," in *Advances in Neural Information Processing Systems*, Z. Ghahramani, M. Welling, C. Cortes, N. Lawrence, and K. Q. Weinberger, Eds., vol. 27. Curran Associates, Inc., 2014.
- [22] X. Sun, L. Liu, Q. Li, J. Dong, E. Lima, and R. Yin, "Deep pixel-to-pixel network for underwater image enhancement and restoration," *IET Image Processing*, vol. 13, no. 3, pp. 469–474, 2019.
- [23] C. Li, S. Anwar, and F. Porikli, "Underwater scene prior inspired deep underwater image and video enhancement,"

- Pattern Recognition*, vol. 98, p. 107038, 2020.
- [24] C. Li, S. Anwar, J. Hou, R. Cong, C. Guo, and W. Ren, "Underwater image enhancement via medium transmission-guided multi-color space embedding," *IEEE Transactions on Image Processing*, vol. 30, pp. 4985–5000, 2021.
- [25] J. Li, K. A. Skinner, R. M. Eustice, and M. Johnson-Roberson, "WaterGAN: Unsupervised generative network to enable real-time color correction of monocular underwater images," *IEEE Robotics and Automation Letters*, vol. 3, no. 1, pp. 387–394, 2017.
- [26] C. Li, J. Guo, and C. Guo, "Emerging from water: underwater image color correction based on weakly supervised color transfer," *IEEE Signal Process. Lett.*, vol. 25, no. 3, pp. 323–327, 3 2018.
- [27] Y. Guo, H. Li, and P. Zhuang, "Underwater image enhancement using a multiscale dense generative adversarial network," *IEEE Journal of Oceanic Engineering*, vol. 45, no. 3, pp. 862–870, 2019.
- [28] M. J. Islam, Y. Xia, and J. Sattar, "Fast Underwater Image Enhancement for Improved Visual Perception," *IEEE Robotics and Automation Letters*, vol. 5, no. 2, pp. 3227–3234, 4 2020. [Online]. Available: <https://ieeexplore.ieee.org/document/9001231/>
- [29] D. P. Kingma and M. Welling, "An Introduction to Variational Autoencoders," *Foundations and Trends® in Machine Learning*, vol. 12, no. 4, pp. 307–392, 2019. [Online]. Available: <http://www.nowpublishers.com/article/Details/MAL-056>
- [30] K. Sohn, H. Lee, and X. Yan, "Learning structured output representation using deep conditional generative models," *Advances in Neural Information Processing Systems (NeurIPS)*, vol. 28, pp. 3483–3491, 2015.
- [31] B. Li, Z. Sun, and Y. Guo, "Supervae: Superpixelwise variational autoencoder for salient object detection," in *Proceedings of the AAAI Conference on Artificial Intelligence (AAAI)*, vol. 33, no. 01, 2019, pp. 8569–8576.
- [32] X. Yan, A. Rastogi, R. Villegas, K. Sunkavalli, E. Shechtman, S. Hadap, E. Yumer, and H. Lee, "Mt-vae: Learning motion transformations to generate multimodal human dynamics," in *Proceedings of the European Conference on Computer Vision (ECCV)*, 2018, pp. 265–281.
- [33] G. Balakrishnan, A. V. Dalca, A. Zhao, J. V. Guttag, F. Durand, and W. T. Freeman, "Visual deprojection: Probabilistic recovery of collapsed dimensions," in *Proceedings of the IEEE International Conference on Computer Vision (ICCV)*, 2019, pp. 171–180.
- [34] A. Abid and J. Zou, "Contrastive variational autoencoder enhances salient features," *arXiv preprint arXiv:1902.04601*, 2019.
- [35] C. Li, C. Guo, W. Ren, R. Cong, J. Hou, S. Kwong, and D. Tao, "An Underwater Image Enhancement Benchmark Dataset and Beyond," *IEEE Transactions on Image Processing*, vol. 29, pp. 4376–4389, 2020.
- [36] Z. Xiao, Y. Han, S. Rahardja, and Y. Ma, "USLN: A statistically guided lightweight network for underwater image enhancement via dual-statistic white balance and multi-color space stretch," 9 2022. [Online]. Available: <https://arxiv.org/abs/2209.02221v1>
- [37] Z. Fu, W. Wang, Y. Huang, X. Ding, and K.-K. Ma, "Uncertainty Inspired Underwater Image Enhancement," 2022, pp. 465–482. [Online]. Available: https://link.springer.com/10.1007/978-3-031-19797-0_27
- [38] X. Huang and S. Belongie, "Arbitrary style transfer in real-time with adaptive instance normalization," in *Proceedings of the IEEE International Conference on Computer Vision (ICCV)*, 2017, pp. 1501–1510.
- [39] J. Johnson, A. Alahi, and L. Fei-Fei, "Perceptual losses for real-time style transfer and super-resolution," in *European conference on computer vision*, 2016, pp. 694–711.
- [40] M. Jahidul Islam, P. Luo, and J. Sattar, "Simultaneous Enhancement and Super-Resolution of Underwater Imagery for Improved Visual Perception," in *Robotics: Science and Systems XVI*. Corvallis, Oregon, USA: Robotics: Science and Systems Foundation, 7 2020. [Online]. Available: <http://www.roboticsproceedings.org/rss16/p018.pdf>
- [41] A. Saleh, I. H. Laradji, D. A. Konovalov, M. Bradley, D. Vazquez, and M. Sheaves, "A realistic fish-habitat dataset to evaluate algorithms for underwater visual analysis," *Scientific Reports*, vol. 10, no. 1, p. 14671, 12 2020. [Online]. Available: <http://www.ncbi.nlm.nih.gov/pubmed/32887922http://www.pubmedcentral.nih.gov/articlerender.fcgi?artid=PMC7473859https://www.nature.com/articles/s41598-020-71639-x>
- [42] T. Mandel, M. Jimenez, E. Risley, T. Nammoto, R. Williams, M. Panoff, M. Ballesteros, and B. Suarez, "Detection confidence driven multi-object tracking to recover reliable tracks from unreliable detections," *Pattern Recognition*, vol. 135, p. 109107, 3 2023. [Online]. Available: <https://linkinghub.elsevier.com/retrieve/pii/S0031320322005878>
- [43] S. LopezMarcano, E. Jinks, C. A. Buelow, C. J. Brown, D. Wang, B. Kusy, E. Ditría, and R. M. Connolly, "Automatic detection of fish and tracking of movement for ecology," *Ecology and Evolution*, vol. 11, no. 12, pp. 8254–8263, 6 2021. [Online]. Available: <https://onlinelibrary.wiley.com/doi/10.1002/ece3.7656>
- [44] R. Liu, X. Fan, M. Zhu, M. Hou, and Z. Luo, "Real-world underwater enhancement: Challenges, benchmarks, and solutions under natural light," *IEEE Transactions on Circuits and Systems for Video Technology*, vol. 30, no. 12, pp. 4861–4875, 2020.
- [45] M. J. Islam, C. Edge, Y. Xiao, P. Luo, M. Mehtaz, C. Morse, S. S. Enan, and J. Sattar, "Semantic Segmentation of Underwater Imagery: Dataset and Benchmark," <http://arxiv.org/abs/2004.01241>, 2020. [Online]. Available: <http://arxiv.org/abs/2004.01241>
- [46] Z. Wang, A. C. Bovik, H. R. Sheikh, and E. P. Simoncelli, "Image quality assessment: from error visibility to structural similarity," *IEEE transactions on image processing*, vol. 13, no. 4, pp. 600–612, 2004.
- [47] D. M. Chandler, "Most apparent distortion: full-reference image quality assessment and the role of strategy," *Journal of Electronic Imaging*, vol. 19, no. 1, p. 011006, 1 2010. [Online].

- Available: <http://electronicimaging.spiedigitallibrary.org/article.aspx?doi=10.1117/1.3267105>
- [48] W. Xue, L. Zhang, X. Mou, and A. C. Bovik, "Gradient Magnitude Similarity Deviation: A Highly Efficient Perceptual Image Quality Index," *IEEE Transactions on Image Processing*, vol. 23, no. 2, pp. 684–695, 2 2014. [Online]. Available: <http://ieeexplore.ieee.org/document/6678238/>
- [49] K. Panetta, C. Gao, and S. Agaian, "Human-visual-system-inspired underwater image quality measures," *IEEE J. Ocean. Eng.*, vol. 41, no. 3, pp. 541–551, 7 2016.
- [50] J. Ke, Q. Wang, Y. Wang, P. Milanfar, and F. Yang, "MUSIQ: Multi-scale Image Quality Transformer," *Proceedings of the IEEE International Conference on Computer Vision*, pp. 5128–5137, 8 2021. [Online]. Available: <https://arxiv.org/abs/2108.05997v1>
- [51] A. Mittal, R. Soundararajan, and A. C. Bovik, "Making a Completely Blind Image Quality Analyzer," *IEEE Signal Processing Letters*, vol. 20, no. 3, pp. 209–212, 3 2013. [Online]. Available: <http://ieeexplore.ieee.org/document/6353522/>
- [52] C. Li, C. Guo, W. Ren, R. Cong, J. Hou, S. Kwong, and D. Tao, "An underwater image enhancement benchmark dataset and beyond," *IEEE Transactions on Image Processing*, vol. 29, pp. 4376–4389, 2019.
- [53] D. Berman, D. Levy, S. Avidan, and T. Treibitz, "Underwater single image color restoration using haze-lines and a new quantitative dataset," *IEEE transactions on pattern analysis and machine intelligence*, vol. 43, no. 8, pp. 2822–2837, 2020.
- [54] A. Paszke, S. Gross, F. Massa, A. Lerer, J. Bradbury, G. Chanan, T. Killeen, Z. Lin, N. Gimelshein, L. Antiga, A. Desmaison, A. Köpf, E. Yang, Z. DeVito, M. Raison, A. Tejani, S. Chilamkurthy, B. Steiner, L. Fang, J. Bai, and S. Chintala, "PyTorch: An imperative style, high-performance deep learning library," in *Advances in Neural Information Processing Systems*, 2019.
- [55] J. E. Contreras-Reyes and R. B. Arellano-Valle, "Kullback-Leibler divergence measure for multivariate skew-normal distributions," *Entropy*, vol. 14, no. 9, pp. 1606–1626, 2012.
- [56] K. Zuiderveld, "Contrast Limited Adaptive Histogram Equalization," in *Graphic Gems IV*. San Diego: Academic Press Professional, 1994, pp. 474–485.
- [57] Y.-T. Peng and P. C. Cosman, "Underwater Image Restoration Based on Image Blurriness and Light Absorption," *IEEE Transactions on Image Processing*, vol. 26, no. 4, pp. 1579–1594, 4 2017. [Online]. Available: <http://ieeexplore.ieee.org/document/7840002/>
- [58] D. Huang, Y. Wang, W. Song, J. Sequeira, and S. Mavromatis, "Shallow-water image enhancement using relative global histogram stretching based on adaptive parameter acquisition," in *International conference on multimedia modeling*, 2018, pp. 453–465.
- [59] X. Chen, P. Zhang, L. Quan, C. Yi, and C. Lu, "Underwater Image Enhancement based on Deep Learning and Image Formation Model," 1 2021. [Online]. Available: <https://arxiv.org/abs/2101.00991v2>
- [60] P. K. Sharma, I. Bisht, and A. Sur, "Wavelength-based Attributed Deep Neural Network for Underwater Image Restoration," *ACM Transactions on Multimedia Computing, Communications, and Applications*, 6 2021. [Online]. Available: <http://arxiv.org/abs/2106.07910>
- [61] D. G. Lowe, "Distinctive Image Features from Scale-Invariant Keypoints," *International Journal of Computer Vision*, vol. 60, no. 2, pp. 91–110, 11 2004. [Online]. Available: <http://link.springer.com/10.1023/B:VISI.0000029664.99615.94>
- [62] H. Li, J. Qin, X. Xiang, L. Pan, W. Ma, and N. N. Xiong, "An Efficient Image Matching Algorithm Based on Adaptive Threshold and RANSAC," *IEEE Access*, vol. 6, pp. 66 963–66 971, 2018. [Online]. Available: <https://ieeexplore.ieee.org/document/8528451/>